Available online at www.sciencedirect.com
SCIENCE DIRECT®
Nuclear Instruments and Methods in Physics Research B 218 (2004) 89–94
NIM B Beam Interactions with Materials & Atoms
www.elsevier.com/locate/nimb

Damage accumulation and amorphization in samarium titanate pyrochlore

Y. Zhang [a,*], V. Shutthanandan [a], R. Devanathan [a], S. Thevuthasan [a], D.E. McCready [a], J. Young [a], G. Balakrishnan [b], D.M. Paul [b], W.J. Weber [a]

[a] *Pacific Northwest National Laboratory, P.O. Box 999, MS K8-93, Richland, WA, 99352, USA*
[b] *Department of Physics, University of Warwick, Coventry, UK*

Abstract

Damage accumulation in $Sm_2Ti_2O_7$ single crystals irradiated with Au^{2+} ions at 170, 300 and 700 K was studied by Rutherford backscattering spectrometry using a 2.0 MeV He^+ beam along the $\langle 0\,0\,1\rangle$ channeling direction. The relative disorder on the Sm sublattice follows a nonlinear dependence on ion fluence. The nonlinear behavior is described well by a disorder accumulation model that indicates a predominant role of a defect-stimulated amorphization process. The critical dose for amorphization at 300 K is ~0.14 dpa, which is in good agreement with in situ transmission electron microscopy results for polycrystalline $Sm_2Ti_2O_7$ irradiated with 600 keV Bi^+ ions and with $Gd_2Ti_2O_7$ doped with ^{244}Cm. Despite the six orders of magnitude difference in damage rates, the good agreement between the amorphization doses in $Sm_2Ti_2O_7$ at 300 K and ^{244}Cm-doped $Gd_2Ti_2O_7$ at 340 K indicates that damage accumulation at these temperatures is relatively independent of dose rate.

PACS: 61.80.Az; 61.80.Jh; 61.82.Ms
Keywords: Damage accumulation; Amorphization; Samarium titanate pyrochlore; Irradiation; Rutherford backscattering spectroscopy

1. Introduction

Materials of composition $A_2B_2O_7$ with the pyrochlore structure have remarkable elemental versatility, which makes these materials of considerable interest for the immobilization of actinide-rich nuclear waste [1–3]. As a result of alpha-decay, actinide-bearing phases will be subjected to considerable self-radiation damage. Radiation damage from alpha-decay can result in amorphization, macroscopic swelling and order-of magnitude increases in dissolution rates [4–7], and these structural changes significantly affect the long-term performance of nuclear waste forms [8–10]. Studies of amorphization in actinide-doped pyrochlores due to the gradual accumulation of alpha-recoil collision cascades can be time consuming [5,6], and only limited data under a few sets of experimental conditions have been obtained. Heavy-ion irradiation studies have been used to more rapidly evaluate radiation effects in a

* Corresponding author. Tel.: +1-509-376-3429; fax: +1-509-376-5106.
E-mail address: yanwen.zhang@pnl.gov (Y. Zhang).

0168-583X/$ - see front matter © 2003 Elsevier B.V. All rights reserved.
doi:10.1016/j.nimb.2003.12.003

wide range of pyrochlore compositions [2,7,11–14], and the results are generally consistent with the behavior in actinide-doped pyrochlores and natural minerals. Results on amorphization, crystal swelling and dissolution rates in ion-beam irradiated materials may provide a reasonable representation of the worst-case effect of radiation effects on chemical and physical durability in actual actinide-containing waste forms over long time periods.

A number of studies have used transmission electron microscopy (TEM) to characterize the critical amorphization dose and the critical temperature for amorphization in ion-irradiated pyrochlores [2,11–14]. Most of these irradiation studies have determined the critical amorphization dose as a function of temperature in polycrystalline materials using in situ TEM. Due to difficulties to grow high-quality single crystals, few studies have quantitatively investigated the damage accumulation behavior as a function of irradiation dose and temperature in order to determine the mechanism for amorphization in titanate pyrochlores. In the current study, irradiation with Au ions is used to simulate alpha-recoil damage in samarium titanate pyrochlore ($Sm_2Ti_2O_7$) single crystal that is characterized by channeling Rutherford backscattering spectrometry (RBS) to achieve a better understanding of damage accumulation processes, which is essential to predict long-term performance of $A_2B_2O_7$ pyrochlores for the immobilization of actinides.

2. Experimental procedures

The $Sm_2Ti_2O_7$ single crystal was grown by a floating zone technique using an IR image furnace at the University of Warwick, UK [15]. The pyrochlore crystal was sectioned along the (1 0 0) plane, and the samples were then polished to 7° between the surface normal and the $\langle 0\,0\,1\rangle$ direction for the irradiation experiments. The Au irradiation and the subsequent ion-beam analysis were carried out using the 3.0 MV tandem accelerator facility within Environmental Molecular Sciences Laboratory (EMSL) at the Pacific Northwest National Laboratory (PNNL) [16]. The $Sm_2Ti_2O_7$ single crystals were irradiated at normal incident to the surface with 1 MeV Au^{2+} ions at 170, 300 and 700 K to ion fluences from 1.0×10^{12} to 8.0×10^{13} cm^{-2}. The damage evolution was characterized by RBS using a 2.0 MeV He^+ beam along the $\langle 0\,0\,1\rangle$ channeling direction. The amorphous state is defined as achieving a relative disorder of 1.0, where the crystalline structure is so highly disordered that the resulting aligned backscattering yield coincides with the random level.

The microstructural features in polycrystalline $Sm_2Ti_2O_7$ under 0.6 MeV Bi^+ irradiation have also been studied by in situ selected area electron diffraction (SAED) over a temperature range from 30 to 950 K. The work was performed using in situ TEM at the HVEM-Tandem facility at Argonne National Laboratory. The critical ion fluence for complete amorphization at each temperature was determined by the loss of all crystalline diffraction maxima.

3. Results and discussion

Damage accumulation under 1.0 MeV Au^{2+} irradiation was analyzed by RBS channeling along the $\langle 0\,0\,1\rangle$ direction. The depth profiles of the relative Sm disorder are derived from each RBS spectrum using an iterative procedure [17,18], and the results of the 300 K irradiation are shown in Fig. 1. The stopping powers for He ions in $Sm_2Ti_2O_7$ from the Stopping and Range of Ions in Matter (SRIM-2003) code [19] have been used to determine the depth scale, using a theoretical density of 6.305 $g\,cm^{-3}$. The stopping powers of He in aligned directions are assumed to be the same as in the random direction due to the uncertainty in establishing the differences. As shown in Fig. 1, the emergence of the damage peak at low dose indicates the presence of disorder due to irradiation, and the increase in disorder with increasing ion fluences is clearly evident. The implantation-induced disorder profile has a peak located at about 100 nm, and full amorphization at the damage peak is observed for a fluence of 4×10^{13} cm^{-2}. Once the peak height is near the random level, the width of the damage peak begins to increase with further irradiation.

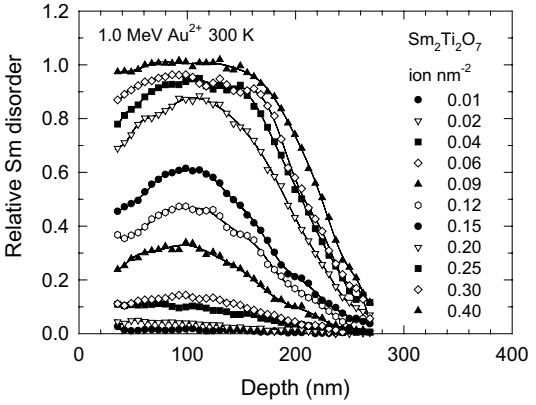

Fig. 1. Depth profiles of the relative Sm disorder. The $Sm_2Ti_2O_7$ single crystal samples were irradiated at 300 K with 1.0 MeV Au^{2+} at normal incident to ion fluences from 1.0×10^{12} to 4×10^{13} cm^{-2}.

For each ion fluence, the local dose at the damage peak, in displacements per atom (dpa), was determined using the SRIM-2003 code [19] under full-cascade mode and assuming a theoretical density of 6.305 $g\,cm^{-3}$ and threshold displacement energies of 50 eV for Sm, Ti and O atoms [4]. The conversion factor at the damage peak from ion fluence (10^{14} cm^{-2}) to local dose (dpa) is 0.45 under the irradiation conditions of this study. Using the local dose and the results in Fig. 1, the damage accumulation can be quantified, as shown in Fig. 2(a). The results indicate that the atomic disorder on the Sm sublattice increases nonlinearly with dose, eventually achieving a fully amorphous state.

According to a disorder accumulation model [20], the total disorder, S, produced under ion-beam irradiation and measured by ion-channeling methods is given by

$$S = f_a + S_d, \tag{1}$$

where f_a is the contribution from irradiation-induced amorphization and S_d is from irradiation-induced disorder in the residual crystalline regions. The amorphous fraction is defined using a direct-impact, defect-stimulated (DI/DS) model for amorphization [21]. In this model, amorphous nuclei are directly produced in the core of a cascade, and the irradiation-induced point defects accumulate and stimulate further amorphization

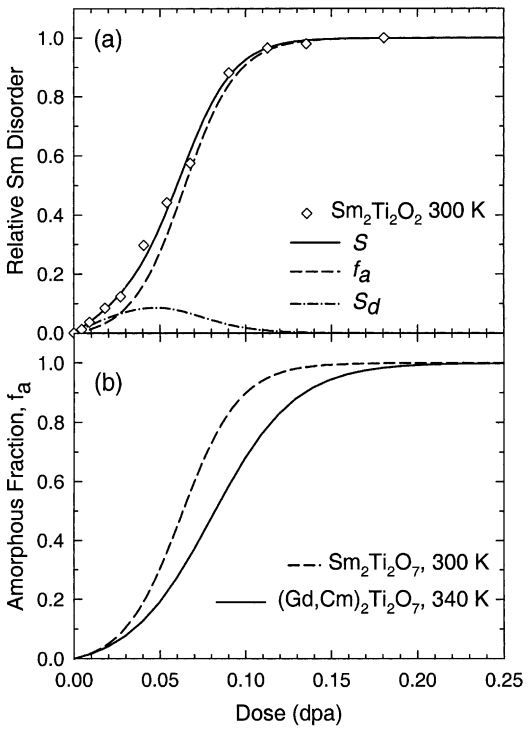

Fig. 2. (a) Relative Sm disorder at the damage peak as a function of local dose for $Sm_2Ti_2O_7$ single crystals irradiated by 1.0 MeV Au^{2+} at 300 K. Solid line is the fit to the disorder accumulation model with the contributions from amorphous region, f_a (dotted line) and residual crystalline region, S_d (dashed line). (b) Amorphous fraction for $Sm_2Ti_2O_7$ irradiated with 1.0 MeV Au^{2+} ions at 300 K and for $Gd_2Ti_2O_7$ doped with 3 wt.% ^{244}Cm due to alpha-decay [23].

at the crystalline–amorphous interfaces. The amorphous fraction is given by the expression [21]

$$f_a = 1 - (\sigma_a + \sigma_s)/\{\sigma_s + \sigma_a \exp[(\sigma_a + \sigma_s)D]\}, \tag{2}$$

where σ_a is the amorphization cross-section, σ_s is the effective cross-section for defect-stimulated amorphization and D is the local dose (dpa). The relative disorder S_d is primarily due to the accumulation of interstitial defects and simple defect clusters. The expression for S_d is given by a simple defect accumulation model multiplied by the probability $(1 - f_a)$ for a defect being produced in the residual crystalline material [22]:

$$S_d = S_d^*[1 - \exp(-BD)](1 - f_a), \tag{3}$$

where S_d^* is the saturation value for the defect-induced disorder and B is proportional to an

effective recombination volume for the specific defects giving rise to S_d.

The solid line in Fig. 2(a) is a fit of the disorder accumulation model (Eq. (1)) to the data, and the contributions from f_a and S_d are illustrated. The fitting parameters are listed in Table 1. As shown in Fig. 2(a), the amorphous fraction, f_a, is a dominant contributor to the total disorder at doses higher than 0.05 dpa. Based on the fit of the disorder accumulation model, the significantly larger value for σ_s relative to σ_a indicates that defect-stimulated amorphization is a primary mechanism leading to amorphization in $Sm_2Ti_2O_7$ at 300 K.

The dependence of f_a on alpha-decay dose at 340 K has been derived from macroscopic swelling data and changes in unit cell volume for $Gd_2Ti_2O_7$ doped with 3 wt.% ^{244}Cm [23]. The results are compared in Fig. 2(b) with the amorphous fraction determined for the Au-irradiated $Sm_2Ti_2O_7$ at 300 K. Although the density of damage energy deposition at the damage peak region from the Au ions in $Sm_2Ti_2O_7$ is about 15% higher than that from alpha recoils in $Gd_2Ti_2O_7$, the amorphization behavior for $Sm_2Ti_2O_7$ has a dependence on dose that is similar to that for ^{244}Cm-doped $Gd_2Ti_2O_7$ at 340 K.

Table 1
Model parameters from fits of Eq. (1) to data in Fig. 2(a)

σ_s (dpa^{-1})	σ_s (dpa^{-1})	S_d^*	B (dpa^{-1})
1.0	63.6	0.30	10

The critical dose for amorphization in $Sm_2Ti_2O_7$ under 0.6 MeV Bi^+ irradiation was studied by in situ TEM over the temperature range from 30 to 950 K. The SAED patterns obtained from samples irradiated at 950 K are shown in Fig. 3, which is representative of the general amorphization behavior observed at lower temperature irradiations. For this TEM study, the dpa was determined at a depth of 30 nm, which is the region that becomes amorphous last and is unaffected by near-surface effects. The pyrochlore crystal structure, as shown by the diffraction pattern in Fig. 3(a), gradually amorphizes with increasing dose. As illustrated in Figs. 3(b) and (c), the intense diffraction spots begin to fade and amorphous halos appear in the SAED patterns. Eventually, all the diffraction spots vanish and only the amorphous halos remain in Fig. 3(d).

The critical dose for amorphization in $Sm_2Ti_2O_7$ under irradiation with 1.0 MeV Au^{2+}

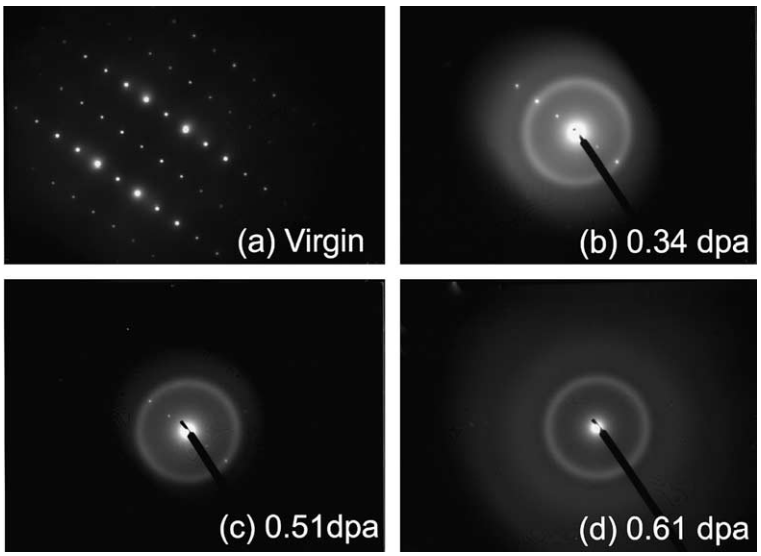

Fig. 3. Diffraction patterns of pyrochlore $Sm_2Ti_2O_7$ irradiated with 0.6 MeV Bi^+ at 950 K. (a) Original, (b) 0.34 dpa, (c) 0.51 dpa and (d) 0.61 dpa.

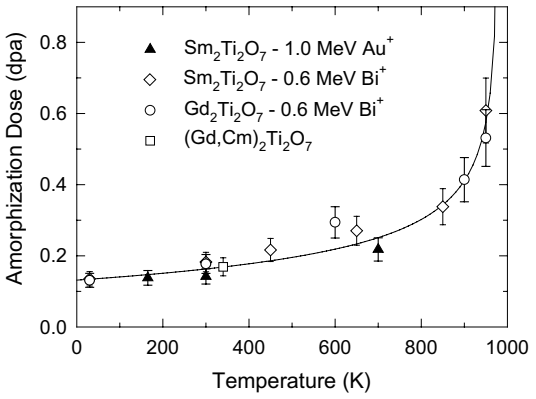

Fig. 4. Critical dose for amorphization of $Sm_2Ti_2O_7$ and $Gd_2Ti_2O_7$ irradiated by 1.0 MeV Au^{2+} and 0.6 MeV Bi^+. Also included is the previous result of critical dose for amorphization in $Gd_2Ti_2O_7$ doped with 3 wt.% ^{244}Cm. The solid line is the best fit to the experimental data.

and 0.6 MeV Bi^+ [4,20] is shown in Fig. 4 as a function of temperature. Also included are the TEM results for $Gd_2Ti_2O_7$ irradiated with 0.6 MeV Bi^+ [4] and due to alpha-decay [23]. In the RBS data, an f_a value of 0.99 was chosen to define the critical amorphization dose. Considering the uncertainties in defining the irradiation dose and amorphous state by RBS and TEM techniques, the results in Fig. 4 indicate a consistent behavior by the two techniques. The critical temperature for amorphization, as shown in Fig. 4, is close to 975 K, which is similar to the onset temperature for the thermal recrystallization of Cm-doped $Gd_2Ti_2O_7$ [6]. It is worth noting that the irradiation studies (characterized by both RBS and TEM) accelerate the damage rates by orders of magnitude compared with the 3 wt.% ^{244}Cm-doped $Gd_2Ti_2O_7$. Despite the six orders of magnitude difference in damage rates, the good agreement between the amorphization doses in $Sm_2Ti_2O_7$ and $Gd_2Ti_2O_7$ under heavy-ion irradiation and in $Gd_2Ti_2O_7$ due to ^{244}Cm decay, as shown in Fig. 4, indicates that amorphization at room temperature under these irradiation conditions is relatively independent of dose rate. The results in Fig. 4 provide some validation for applying models of damage accumulation and amorphization under heavy-ion irradiation in rare-earth titanates to predict long-term behavior due to alpha-decay.

4. Conclusions

In the current study, single crystal $Sm_2Ti_2O_7$ was irradiated with 1 MeV Au^{2+} to simulate the alpha-recoil damage. The damage accumulation on the Sm sublattice indicates a nonlinear behavior as a function of ion dose. Based on a model fit, defect-stimulated amorphization is the primary mechanism leading to amorphization in $Sm_2Ti_2O_7$. The critical dose for amorphization under 1.0 MeV Au^{2+} irradiation in the $Sm_2Ti_2O_7$ crystal is in good agreement with TEM results for polycrystalline $Sm_2Ti_2O_7$ and $Gd_2Ti_2O_7$ under 0.6 MeV Bi^+ irradiation and for ^{244}Cm-doped $Gd_2Ti_2O_7$, indicating that amorphization due to heavy-ion energy deposition is relatively independent of dose rate at about room temperature. As a result, the model of damage accumulation and amorphization under heavy-ion irradiation in rare-earth titanates can be used to predict long-term behavior due to alpha-decay.

Acknowledgements

This work was supported by the Division of Materials Sciences & Engineering, Office of Basic Energy Sciences, US Department of Energy. Support for the accelerator facilities within the Environmental Molecular Sciences Laboratory (EMSL) was provided by the Office of Biological and Environmental Research, US. The Pacific Northwest National Laboratory is operated by Battelle Memorial Institute for the US Department of Energy under Contract DE-AC06-76RLO 1830.

References

[1] K.E. Sickafus, L. Minervini, R.W. Grimes, J.A. Valdez, M. Ishimaru, F. Li, K.J. McClellan, T. Hartmann, Science 289 (2000) 748.
[2] S.X. Wang, B.D. Begg, L.M. Wang, R.C. Ewing, W.J. Weber, K.V. Govidan Kutty, J. Mater. Res. 14 (1990) 4470.
[3] A.B. Harker, in: W. Lutze, R.C. Ewing (Eds.), Radioactive Waste Forms for the Future, North-Holland, Amsterdam, 1988, p. 335.
[4] B.D. Begg, N.J. Hess, W.J. Weber, R. Devanathan, J.P. Icenhower, S. Thevuthasan, B.P. McGrail, J. Nucl. Mater. 288 (2001) 208.

[5] W.J. Weber, J.W. Wald, H.J. Matzke, Mater. Lett. 3 (1985) 173.
[6] W.J. Weber, J.W. Wald, H.J. Matzke, J. Nucl. Mater. 138 (1986) 196.
[7] B.D. Begg, W.J. Weber, R. Devanathan, J.P. Icenhower, S. Thevuthasan, B.P. McGrail, Ceram. Trans. 107 (2000) 553.
[8] R.C. Ewing, W.J. Weber, W. Lutze, in: E.R. Merz, C.E. Walter (Eds.), Diposal of Weapon Plutonium, Kluwer Academic Publishers, The Netherlands, 1996, p. 65.
[9] R.C. Ewing, W.J. Weber, F.W. Clinard Jr., Prog. Nucl. Energy 29 (1995) 63.
[10] W.J. Weber, R.C. Ewing, C.R.A. Catlow, T. Diaz de la Rubia, L.W. Hobbs, C. Kinoshita, H.J. Matzke, A.T. Motta, M. Nastasi, E.K.H. Salje, E.R. Vance, S.J. Zinkle, J. Mater. Res. 13 (1998) 1434.
[11] R.C. Ewing, L.M. Wang, Nucl. Instr. and Meth. B 65 (1992) 319.
[12] S.X. Wang, L.M. Wang, R.C. Ewing, G.S. Was, G.R. Lumpkin, Nucl. Instr. and Meth. B 148 (1999) 704.
[13] S.X. Wang, L.M. Wang, R.C. Ewing, K.V. Govidan Kutty, in: S.J. Zinkle, G.E. Lucas, R.C. Ewing, J.S. Williams (Eds.), Microstructural Processes in Irradiated Materials, Mater. Res. Soc. Sympos. Proc. 540 (1999) 355.
[14] W.J. Weber, N.J. Hess, Nucl. Instr. and Meth. B 80–81 (1993) 1245.
[15] G. Balakrishnan, O.A. Petrenko, M.R. Lees, D.M. Paul, J. Phys.: Condens. Matter 10 (1998) L723.
[16] S. Thevuthasan, C.H.F. Peden, M.H. Engelhard, D.R. Baer, G.S. Herman, W. Jiang, Y. Liang, W.J. Weber, Nucl. Instr. and Meth. A 420 (1999) 81.
[17] M.L. Swanson, in: J.R. Tesmer, M. Nastasi (Eds.), Handbook of Modern Ion Beam Materials Analysis, Materials Research Society, Pittsburgh, PA, 1995, p. 263.
[18] J.S. Williams, R.G. Elliman, in: J.R. Bird, J.S. Williams (Eds.), Ion Beams for Materials Analysis, Academic Press, Australia, 1989, p. 286.
[19] J.F. Ziegler, J.P. Biersack, U. Littmark, The Stopping and Range of Ions in Solids, Pergamon, New York, 1985.
[20] Y. Zhang, W.J. Weber, V. Shutthanandan, R. Devanathan, S. Thevuthasan, G. Balakrishnan, D.M. Paul, J. Appl. Phys., in press.
[21] W.J. Weber, Nucl. Instr. and Meth. B 166–167 (2000) 98.
[22] Y. Zhang, W.J. Weber, W. Jiang, A. Hallén, G. Possnert, J. Appl. Phys. 91 (2002) 6388.
[23] W.J. Weber, R.C. Ewing, in: B.P. McGrail, G.A. Cragnolino (Eds.), Scientific Basis for Nuclear Waste Management XXV, Mater. Res. Soc. Sympos. Proc. 713 (2002) 443.